Nuclear Engineering and Technology 52 (2020) 2431–2441

Contents lists available at ScienceDirect

Nuclear Engineering and Technology

journal homepage: www.elsevier.com/locate/net

Original Article

Development and verification of pin-by-pin homogenized simplified transport solver Tortin for PWR core analysis

Petra Mala [a, b, *], Andreas Pautz [a, b]

[a] Ecole Polytechnique Federale de Lausanne, Station 9, Lausanne, Switzerland
[b] Paul Scherrer Institute, Forschungstrasse 111, 5232, Villigen, Switzerland

ARTICLE INFO

Article history:
Received 19 December 2019
Received in revised form
20 March 2020
Accepted 22 April 2020
Available online 27 April 2020

Keywords:
Pin-by-pin
Superhomogenization
MOX
Spatial discretization
Microscopic depletion

ABSTRACT

Currently, the pin-by-pin homogenized solvers are a very active research field as they can, unlike the nodal codes, directly predict the local power, while requiring significantly less computational resources than the heterogeneous transport codes. This paper presents a recently developed pin-by-pin diffusion/SP3 solver Tortin, its spatial discretization method and the reflector treatment. Regarding the spatial discretization, it was observed that the finite difference method applied on pin-cell size mesh does not properly capture the big flux change between MOX and uranium fuel, while the nodal expansion method is more accurate but too slow. If the finite difference method is used with a finer mesh in the outer two pin rows of the fuel assembly, it increases the required computation time by only 50%, but decreases the pin power errors below 1% with respect to lattice code reference solutions. The paper further describes the coupling of Tortin with a microscopic depletion solver. Several verification tests show that the SP3 pin-by-pin solver can reproduce the heterogeneous transport solvers results with very good accuracy, even for fuel cycle depletion of very heterogeneous core employing MOX fuel or inserted control rods, while being two orders of magnitude faster.

1. Introduction

A key element of nuclear reactor core-oversight procedures is the recurrent neutronics calculation for the core-reload licensing. The currently used neutronic solvers are based on a two-step approach, where the homogenized few-group cross sections are generated from single-assembly 2D transport calculations and then used in a 3D nodal (assembly-wise) core solver. The increasing complexity of modern reactor core designs necessitates increasingly accurate computational techniques, since the cross sections homogenized for single assembly with reflective boundary conditions cause significant errors on assembly interfaces with strong spectral and spatial gradients (e.g. MOX, fuel with high burnup, assembly/reflector interfaces). To decrease this error, recent nodal solvers often do a spectral rehomogenization of the nodal cross sections with a flux obtained in a calculation with more realistic boundary conditions [1,2]. Another possibility is employing core solvers with higher spatial resolution, e.g. pin-cell-wise (when we speak of pin cell here, we always refer to homogenized pin cells, i.e. where fuel, cladding, and coolant are homogenized, as opposed to the heterogeneous picture, in which the fuel rod geometry is preserved). Although many such codes have been developed [3–7], the published results show often only little gain in accuracy over nodal codes [8].

One of the problems is that the pin-by-pin codes have difficulties to reproduce the heterogeneous solutions on MOX/uranium assembly interfaces [4,6]. Several methods have been developed to decrease this error, mostly based on parametrization of the cross sections or discontinuity factors for the neighboring environment (assemblies or pins). For real reactor applications, the parametrization can require many lattice code calculations of e.g. 3x3 assembly problems to represent well all the possible configurations with different assemblies and burnups. This can be rather expensive for possible industrial applications [7]. To our knowledge, none of these methods has been extensively used for depletion studies.

The errors of the homogenized core solvers in comparison to a fully heterogeneous solution are caused by spatial homogenization and group collapsing, transport approximation, and spatial discretization. The core solvers usually employ diffusion or simplified transport method (SP3), which use the diffusion

* Corresponding author. Ecole Polytechnique Federale de Lausanne, Station 9, Lausanne, Switzerland.
E-mail address: petra.mala@psi.ch (P. Mala).

https://doi.org/10.1016/j.net.2020.04.022

coefficient to approximate the transport effects. Since the quality of the results depends severely on the diffusion coefficients and since the lattice codes use different approximations to calculate them, two lattice codes were used in this work. The same code was consistently used in order to generate the cross sections for the pin-by-pin calculation, and to provide the reference solution. By doing so, one avoids entirely any discrepancies coming from nuclear data libraries or lattice solver approximations, which are not part of this investigation.

For the fuel cycle analysis, the lattice code depletes each assembly under certain nominal operating conditions. In a real reactor, the neutron spectrum and consequently the fuel isotopic composition can vary significantly from the nominal one. This so-called spectral history effect is in the nodal codes usually taken into account by history-averaged cross sections [9], spectral indexes [10], concentration of Pu239 [11], or hybrid micro/macroscopic depletion [12]. The first three methods are approximative techniques able to capture quite well the spectral history effect of different fuel and moderator temperatures and boron concentration on actinides composition.

However, they are not able to accurately model operation on lower power or with partially inserted control rods. Under these conditions, it is necessary to precisely calculate the fission products. Therefore, the recent nodal codes often explicitly calculate concentration of about 60–80 most important nuclides [1,12]. This is becoming even more important with Generation III+ reactors, which are expected to be operational for load-following. The spectral history effect is likely to be even more pronounced in the pin-by-pin calculations than in the nodal ones, which averages the deviations over the whole assembly.

In this paper, a newly conceived pin-by-pin diffusion/SP3 solver Tortin [13] is presented and verified against the heterogeneous method of characteristics and Monte Carlo codes. The calculations were done for a 2D 2x2 assembly minicore with very heterogeneous fuel configuration and for 2D quarter cores without and with inserted control rods. Then, the code Tortin was coupled with the microscopic depletion solver Ventina [14]. Since Ventina has been developed only recently, at first a few verification tests are shown, followed by a few pin-by-pin fuel cycle calculations.

2. Methodology and codes

2.1. Pin-by-pin solver Tortin

The pin-by-pin code employed in this work was Tortin. It can solve diffusion or SP3 equations in 3D. The finite difference method is used for the spatial discretization, which leads to a matrix with only a few non-zero diagonals. Two matrix solvers can be used, a direct solver PARDISO [15] and an iterative solver based on the BiCGstab method with a multigrid preconditioner [16]. The direct solver is faster for small problems. The Chebychev method is used to accelerate the outer iterations.

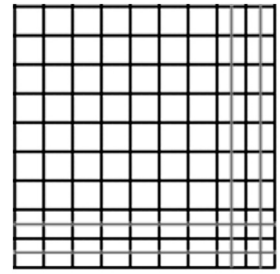

Fig. 1. Discretization scheme of Tortin for quarter assembly.

The finite difference discretization was observed not to be sufficient to capture the flux gradients on the MOX/uranium and fuel/reflector interfaces. Therefore, Tortin uses a finer mesh with two points per cell in the two outer rows of each assembly, as depicted in Fig. 1. For these calculations, the cross sections are still homogenized for each pin cell and the SPH factors are also pin cell wise, but they have to be calculated with the finer mesh (the same mesh must be used when calculating the SPH factors and when applying them in the core calculations) and averaged for the given pin cell.

The SP3 module solves the following set of diffusion-like equations:

$$-D_{1,g}\nabla^2(\phi_{0,g}+2\phi_{2,g})+\Sigma_{r,g}(\phi_{0,g}+2\phi_{2,g})=\frac{\chi_g}{k}\sum_{g'}\nu\Sigma_{f,g'}\phi_{0,g'}+\sum_{g'\neq g}\Sigma_{s,g'\to g}\phi_{0,g'}+2\Sigma_{r,g}\phi_{2,g}$$
$$-\frac{9}{5}D_{3,g}\nabla^2\phi_{2,g}+\Sigma_{t,g}\phi_{2,g}=\frac{2}{5}\left\{\Sigma_{r,g}\phi_{0,g}-\frac{\chi_g}{k}\sum_{g'}\nu\Sigma_{f,g'}\phi_{0,g'}+\sum_{g'\neq g}\Sigma_{s,g'\to g}\phi_{0,g'}\right\} \quad (1)$$

where the diffusion coefficient

$$D_l=\frac{1}{(2l+1)\Sigma} \quad (2)$$

where $\Sigma=\Sigma_{tr}$ for $l=1$ and $\Sigma=\Sigma_t$ for $l=3$.

In (1), g is the energy group, ϕ_0 and ϕ_2 are the scalar flux and the second moment of the flux, Σ_r is the removal, Σ_f the fission, Σ_s the scattering, and Σ_t the total macroscopic cross section, ν is the fission yield, χ is the fission spectrum, k is the multiplication factor, and Σ_{tr} is the transport cross section.

The diffusion (SP1) module solves the first equation only by setting $\phi_2=0$.

2.2. Lattice codes

The transport cross section is used in diffusion and SP3 solvers to account for the anisotropy. It should be consistently calculated as

$$\Sigma_{tr}^g=\Sigma_t^g-\frac{\sum_{g'}\Sigma_{s1}^{g'\to g}\phi_1^{g'}}{\phi_1^g} \quad (3)$$

where $\phi_1^{g'}$ and ϕ_1^g are the first flux moments in energy groups g' and g, respectively, Σ_t is the total cross section and Σ_{s1} the P1 scattering cross section.

This so-called inscatter approximation has two main problems:

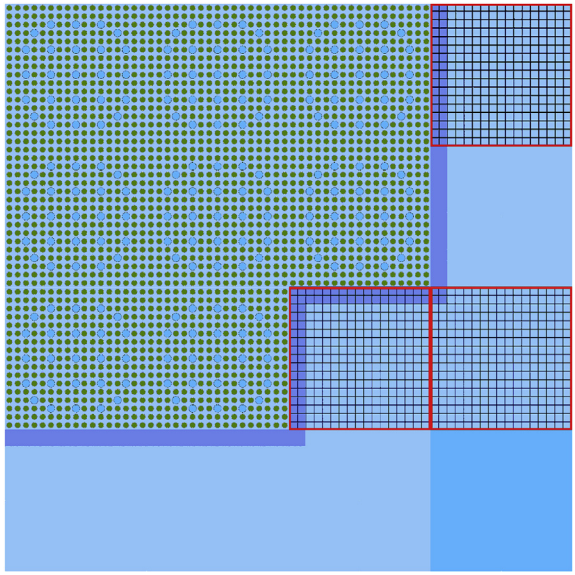

Fig. 2. Configuration for reflector cross section generation.

first, many lattice codes (method of characteristics, Monte Carlo) simply do not provide the first flux moment needed. Some codes, in particular CASMO [17], approximate it by solving the P_N equation for a homogeneous slab of water of infinite thickness for a uniform fission spectrum source [18]. Monte Carlo codes often use the cumulative migration method [19]. The second problem is that the method can yield negative values as the first flux moment can be in principle negative. Therefore another, the so-called outscatter approximation was suggested, leading to

$$\Sigma_{tr}^{g} = \Sigma_{t}^{g} - \frac{\sum_{g'} \Sigma_{s1}^{g\to g'} \phi_1^g}{\phi_1^g} = \Sigma_{t}^{g} - \sum_{g'} \Sigma_{s1}^{g\to g'} \tag{4}$$

This approximation assumes that the P1 inscatter and outscatter sources are equal, which means that the first flux moments in the fraction cancel out and their knowledge is not required.

Two codes were used in this work to produce the pin cell cross sections, SERPENT and CASMO-5. The Monte Carlo code SERPENT [20] can provide diffusion coefficient with both inscatter and outscatter approximation. The inscatter approximation uses either the cumulative migration method or the energy-dependent transport correction [21]. The implemented cumulative migration method in suitable only for homogenizing over the entire geometry with reflective or periodic boundary conditions [20]. For the pin-cell homogenization, it can produce negative diffusion coefficients. Therefore, the energy-dependent transport correction was used in this work.

CASMO-5 is a method of characteristics (MOC) solver, which can use either the transport corrected total cross sections or it can explicitly use the scattering moments up to P5. At first, the code solves 1D area-equivalent cylindrical pin-cell problems in 586 energy groups and uses the obtained flux to collapse the cross sections in energy. Then, the 2D MOC calculation is performed with the energy collapsed cross sections but in the fully heterogeneous geometry, the cross sections are not collapsed spatially in the 1D pin-cell calculations. In this work, the MOC solver was run in 35 groups and with the P3 scattering source. The inscatter approximation [18] is employed to calculate the diffusion coefficient.

To homogenize the cross sections over each pin cell, both the lattice codes use a simple flux-volume weighting. The super-homogenization (SPH) method [22] was used in this work as an equivalence method between the lattice and the pin-by-pin solver. This is an iterative method which can preserve reaction rates in the pin cells by rescaling the cross sections by so-called SPH factors, which are defined as the ratio of heterogeneous and homogeneous scalar pin cell fluxes. These factors were calculated on the single-assembly-level and for all branches.

All the pin-by-pin calculations were done in 8 groups. The energy boundaries in libraries produced by CASMO-5 and SERPENT are the same (the CASMO default ones).

2.3. Reflector cross section generation

The current nodal codes usually generate the reflector cross sections in "2-assembly" configuration with one assembly being a fuel assembly and the other one being the reflector. When the cross sections are homogenized over the whole reflector region, where the spectrum is rapidly changing, they cannot adequately reproduce the response of the reflector to the core. Therefore, the nodal codes use additional correction techniques [23,24].

For the pin-by-pin solver, the cross sections were generated for each "pin" of a reflector, i.e. the reflector areas were, like the reactor core, subdivided into fuel-cell-sized regions. In case of a baffle reflector (a few cm thick steel with water), three sets of cross sections must be produced for the parts which have side contact with 1, 2, or 0 fuel assemblies, as depicted in Fig. 2.

2.4. Depletion calculations

2.4.1. Ventina

For the depletion calculations, Tortin was coupled with a microscopic depletion solver Ventina [14]. The code solves the set of Bateman equations:

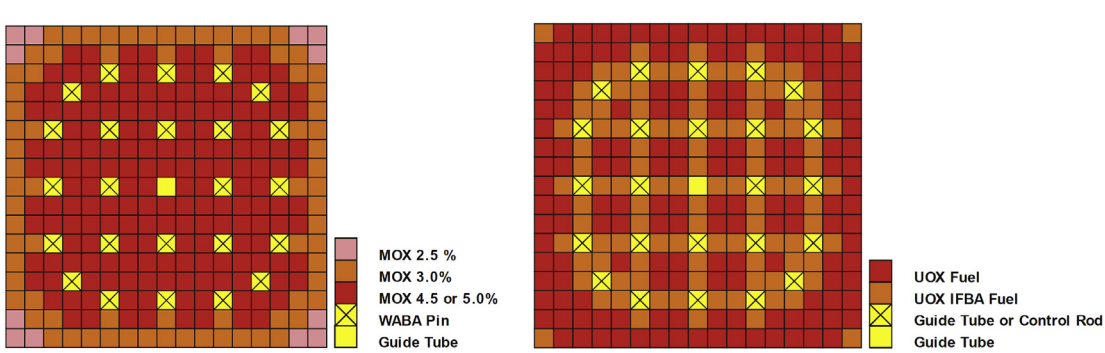

Fig. 3. MOX and uranium assembly layout.

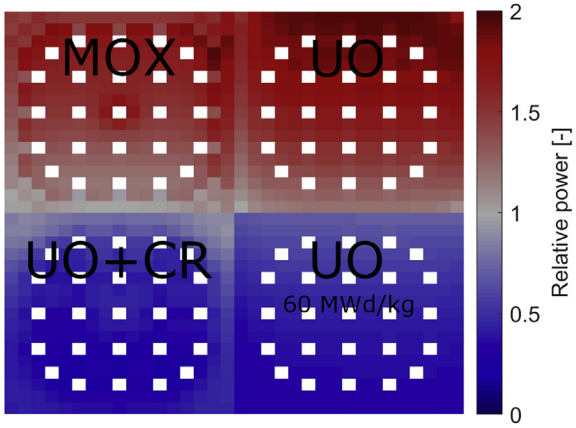

Fig. 4. Pin power distribution calculated by CASMO-5.

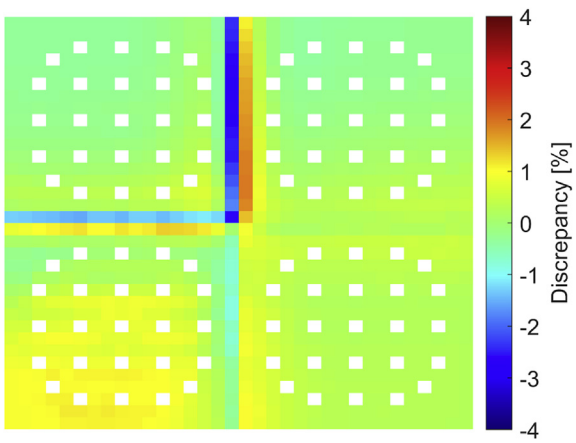

Fig. 5. Pin power error of Tortin SP3 using CASMO-5 cross sections and CASMO-5 reference values.

$$\frac{dN_i}{dt} = \sum_k \lambda_{ki} N_k + \phi \sum_j \gamma_{ji} \sigma_j^f N_j + \phi \sigma_{i-1}^c N_{i-1} - \lambda_i N_i - \phi \sigma_i^a N_i \tag{5}$$

where N_i is the concentration of nuclide i, λ_{ki} is the decay constant of nuclide k to nuclide i, ϕ is the neutron flux, γ_{ji} is the fission yield of nuclide i from the fission of nuclide j, σ^f is the fission cross section, σ^c the capture cross section, λ_i is the decay constant of nuclide i, and σ^a is the absorption cross section. Nuclear data are assumed to remain constant during the depletion step.

Equation set (5) can be written in the following matrix representation:

$$\frac{d\boldsymbol{N}}{dt} = \boldsymbol{AN} \tag{6}$$

where **N** indicates the nuclide vector and **A** the transition matrix. Solution of the set of differential equation (6) has an exponential form

$$\boldsymbol{N}(t) = \exp(\boldsymbol{A}t)\boldsymbol{N}(0) \tag{7}$$

Analytic solution of the matrix exponential is not trivial and numerical methods must be employed for practical use. Several solvers are implemented in Ventina, including the Chebyshev rational approximation method (CRAM) [25], which is the fastest method and was therefore used in this work. In this method, the exponential is converted into a fraction of two Chebyshev polynomials and the solution (7) can then be rewritten as

$$\boldsymbol{N}(t) = \alpha_0 \boldsymbol{N}(0) + 2Re\left[\sum_{i=1}^{k/2} \alpha_i (\boldsymbol{A}t - \theta_i \boldsymbol{I})^{-1}\right]\boldsymbol{N}(0) \tag{8}$$

which converts the problem to obtaining $k/2$ solutions of sets of linear equations (where k is the order of the CRAM approximation). The solver of order 14 has been employed in this work, using the coefficients α and θ precomputed in Ref. [26]. The system of linear equations is solved in Ventina by the LU decomposition.

All the data, i.e. cross sections, decay constants, fission yields, as well as the nuclide chains, were extracted from CASMO-5, in order

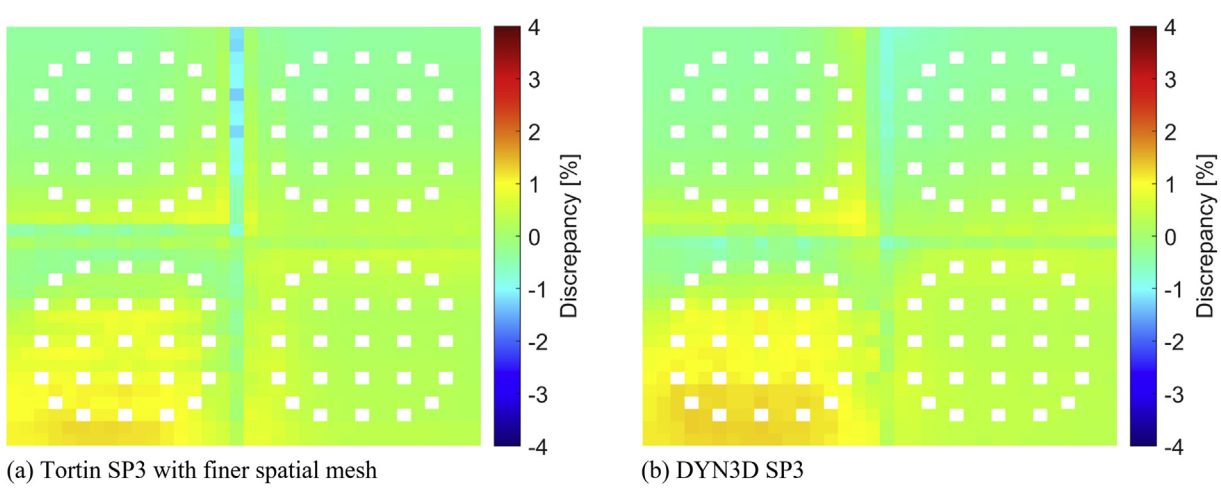

Fig. 6. Pin power error using CASMO-5 cross sections and CASMO-5 reference values.
(a) Tortin SP3 with finer spatial mesh
(b) DYN3D SP3.

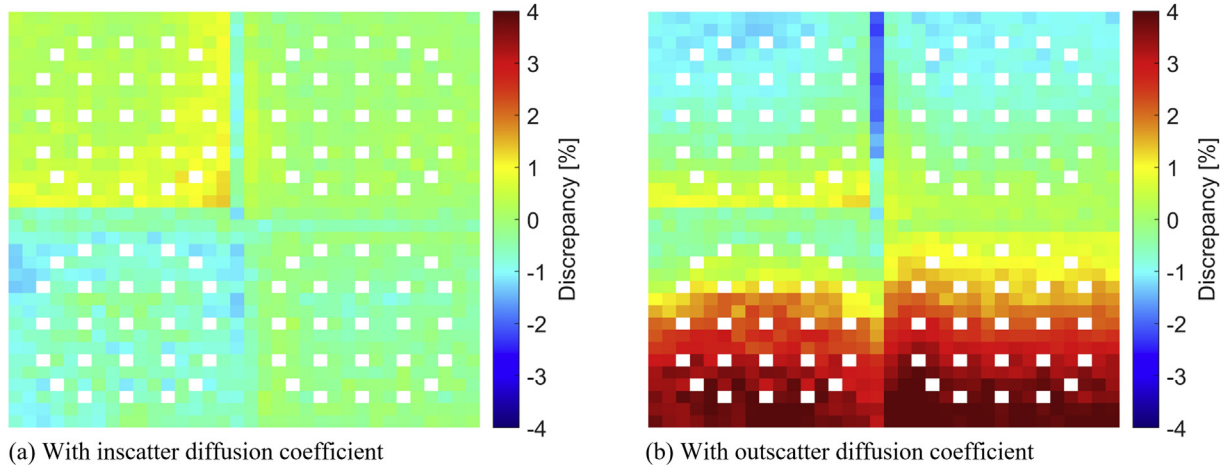

Fig. 7. Pin power error of Tortin SP3 using SERPENT cross sections and SERPENT reference values.
(a) With inscatter diffusion coefficient.
(b) With outscatter diffusion coefficient.

Table 1
Eigenvalue errors for 2x2 assembly problem.

Code	keff [pcm]	Code	keff [pcm]
CASMO	**1.03702**	SERPENT	**1.03494**
Tortin - inscat	−34	Tortin - inscat	−113
		Tortin - outscat	−343

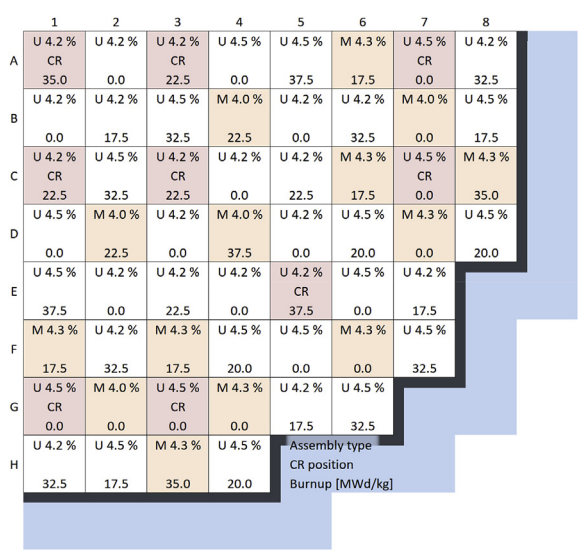

Fig. 8. Quarter core layout.

to ensure maximum consistency between the lattice code and Ventina. The CASMO-5 library used in this work is based on ENDF/B-VII.1 and contains data for more than 300 nuclides.

2.4.2. Depletion calculation scheme

The depletion step length was mostly 0.5 MWd/kg, with additional step of 0.1 MWd/kg after a change of the operating conditions. To decrease the error caused by assumption of constant flux and cross sections during one depletion step, the predictor-corrector technique was used in the following manner:

Table 2
Eigenvalue, pin power errors, and computation wall times for quarter core ('hot pin' is the error of the rod with the highest power).

Case	Code	keff [pcm]	Pin power error RMS [%]	Max [%]	Hot pin [%]	Time [s]
ARO	CASMO	**1.06100**				4400
	Tortin SP3	28	0.59	−1.97	0.30	51
	Tortin SP1	−9	1.65	−4.70	0.20	20
ARI	CASMO	**1.01917**				3100
	Tortin SP3	14	0.56	−1.98	−0.10	34
	Tortin SP1	−87	1.69	−4.73	−0.87	13

- The transport calculation is run for the beginning of the time step t_n
- The flux is used in the depletion calculation and the new nuclide composition for step t_{n+1} is obtained. The macroscopic cross sections are calculated as:

$$\Sigma = \Sigma_{CASMO} + \sigma(N_{VENTINA} - N_{CASMO})$$

- The transport calculation at time t_{n+1} is performed and the average flux for this depletion step is calculated
- The depletion calculation is performed again with the averaged flux and the resulting nuclide composition is used to calculate again the macroscopic cross sections.

A significant part of the computation time is taken by interpolation of the microscopic cross sections. Two interpolation routines have been implemented, multi-linear and multi-cubic. In this work, the four-dimensional (burnup, moderator and fuel temperature, and boron concentration) cubic interpolation was used. (The interpolations can be significantly accelerated by processing together all data for one cell, as all this data are interpolated for the same burnup, temperature, etc. The innermost loop is then done over N_isotopes*N_group*N_xs_types and this loop can be vectorized. The speed up for the four-dimensional cubic interpolation using single precision is about 7. The theoretical maximum speed up would be 8 (256 bit register/32 bit float). The main bottleneck of

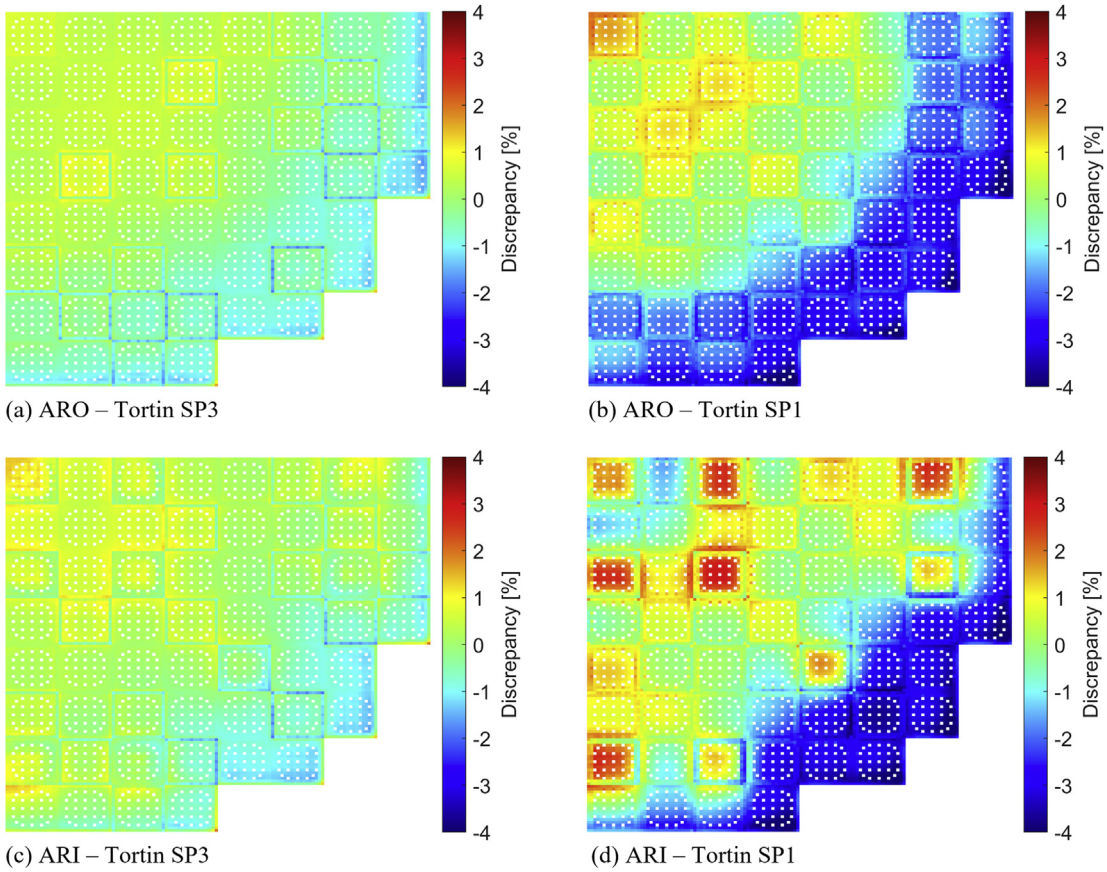

Fig. 9. Pin power error of Tortin for quarter core.
(a) ARO – Tortin SP3 (b) ARO – Tortin SP1
(c) ARI – Tortin SP3 (d) ARI – Tortin SP1.

this routine is the memory access, as all the data required during the collapsing do not fit the L1 cache.)

3. Test case description

The assemblies selected for this study are based on the OECD/NEA PWR MOX/UO_2 benchmark [27]. They have a lattice of 17x17 rods with 25 guide tubes. There are two types of uranium and of MOX assemblies. The uranium assembly contains rods with 4.2% (or 4.5%) enrichment and some rods are coated with the IFBA absorber (Integrated Fuel Burnable Absorber, ZrB_2). 24 control rods can be inserted into the uranium assembly. The MOX assembly is composed of fuel rods with weight fractions of 4.5% (or 5.0%), 3.0% and 2.5% of plutonium and its 24 guide tubes are filled with the WABA absorber (Wet Annular Burnable Absorber, Al_2O_3–B_4C). The layout of assemblies is shown in Fig. 3.

The library was prepared for the following branches (underlined are the nominal conditions):

- Fuel temperature: 560, <u>900</u>, 1320 K
- Moderator temperature: 560, <u>580</u>, 600 K
- Boron concentration: 0, <u>1000</u>, 2000 ppm
- Burnup: 0, 0.1, 0.5, 1, 2, …, 11, 12.5, 15, …, 70 MWd/kg

4. Results for 2x2 assembly problem

The calculations were done first for a 2x2 assembly case with reflective boundary condition. The geometry and the power profile calculated by CASMO-5 are shown in Fig. 4. It is a small problem, but with very high leakage effects and spectral complexity caused by a MOX assembly. Since there is a big power gradient over the domain, the results of diffusion and SP3 solvers are strongly dependent on the diffusion coefficient. The outscatter approximation used in SERPENT overpredicts the diffusion coefficient in the fastest group by about 20%. The inscatter coefficients in the fastest group are similar for both the lattice codes.

The pin power errors of Tortin SP3, employing CASMO-5 cross sections and reference values, are shown in Fig. 5. The errors are very small, except for 2–3% errors on the MOX/uranium interface. The major reason of these errors is the steep flux change, which the finite difference code with pin-size mesh is not able to properly capture. If a finer 2x2 mesh per pin cell is used in the outer-assembly pins, as depicted in Fig. 1, the error drops rapidly to about 1%, as can be seen in Fig. 6.

The results do not get significantly better with even higher number of meshes. However, to complete the study on the spatial discretization, the code DYN3D [8] employing the nodal expansion

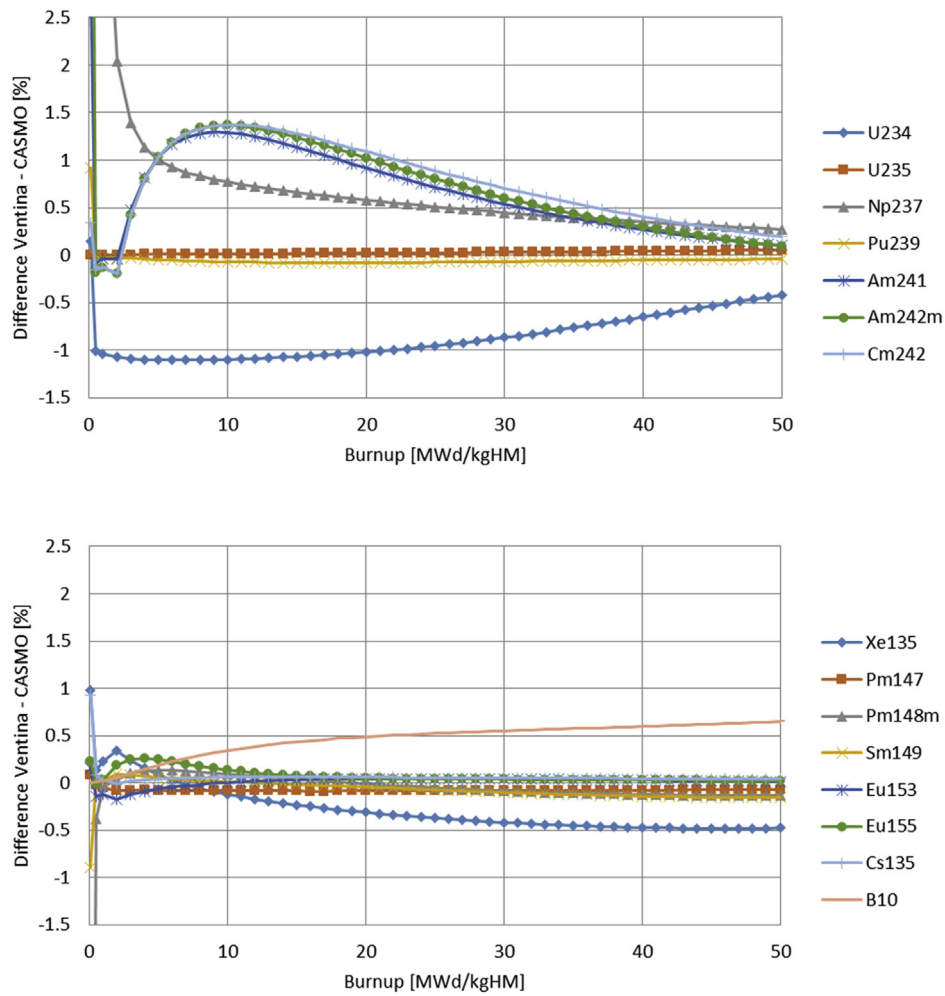

Fig. 10. Nuclide composition difference between Ventina and CASMO-5 for some important actinides (top) and fission products and burnable absorber (bottom) for a uranium fuel pin cell.

method was also used. As can be seen in Fig. 6, the results are of similar quality as the ones obtained with Tortin, but its computation time was about ten times higher.

To show that the pin-homogenized codes can approximate well also a Monte Carlo solution, the same calculation was performed with SERPENT cross sections and the results were compared against SERPENT reference values. The errors are shown in Fig. 7. With the inscatter diffusion coefficient, Tortin can reproduce the SERPENT solution very well, with about 1% error around the MOX/uranium interface, which is in good agreement with the previous results. However, the outscatter diffusion coefficients significantly overpredict the leakage and cause a few percent power error in the assemblies with control rods and burnt fuel.

Table 1 shows the eigenvalues obtained with CASMO-5 and with SERPENT and the errors of Tortin. With the CASMO-5 cross sections, the error of Tortin against CASMO-5 is only 34 pcm. When using the SERPENT cross sections, the errors are higher, in particular with the outscatter diffusion coefficients, which overpredict the leakage.

5. Results for 2D quarter core

To continue the verification of Tortin with a more realistic reactor core problem, two quarter core calculations were performed, for a core configuration based on the MOX/UO2 benchmark with ARO (all rods out) and ARI (all rods in). The layout of the problem is shown in Fig. 8. The core is surrounded by a baffle reflector of assembly-pitch thickness, composed of 2.52 cm of steel followed by water. The calculations were done with Tortin with CASMO-5 cross sections and compared against CASMO-5 reference values.

First calculation was done for the core without inserted control rods. The results are summarized in Table 2. From the pin power error maps shown in Fig. 9, it can be noticed that the biggest errors are in general located in the vicinity of the reflector. In case of Tortin SP3, the errors are very small, with the pin power error RMS of 0.6% and the maximum error below 2%. The biggest errors are in the pins close to the reflector and on the interfaces of uranium and fresh MOX assemblies. The hot pin error is only 0.3%. In case of the Tortin diffusion solver, there is a bigger underprediction of the power in two rows of assemblies around the reflector, with maximum error of 4.7%. There is also about 2% error in or around the assemblies with the highest burnup. The pin power error RMS is 1.65%.

In case of the core with inserted control rods, the errors of Tortin SP3 are again very small with the pin power error RMS of 0.6% and the maximum error of 2% located on the interfaces of uranium and fresh MOX assemblies. The diffusion solver underpredicts the power in the assemblies around the reflector, like in the ARO case. Moreover, it overpredicts the power in the controlled assemblies by about 3%. The pin power error RMS is 1.7%.

Table 2 shows also the computation wall times of the solvers.

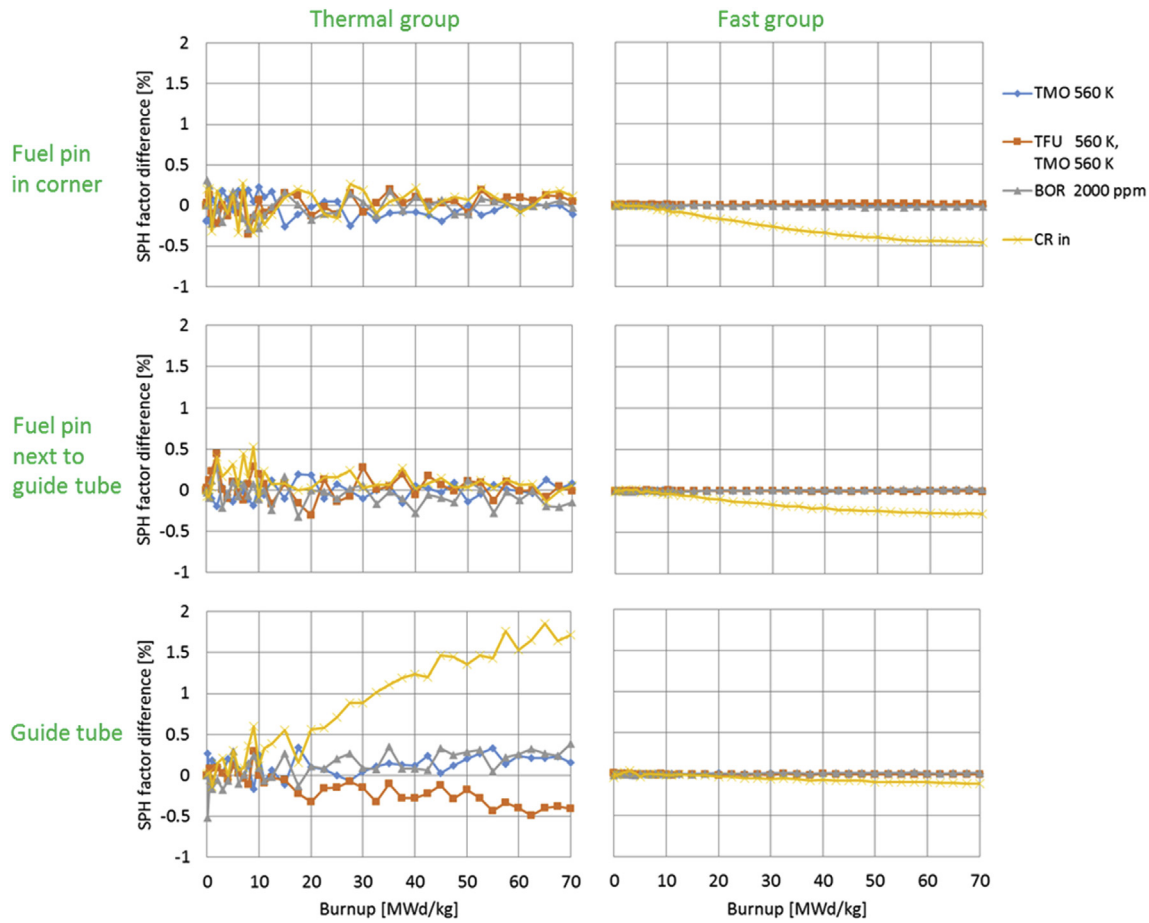

Fig. 11. SPH factors dependence on history variables for fast and thermal energy group of corner fuel pin (top), fuel pin next to guide tube (center), and guide tube (bottom).

The SP3 solver of Tortin needs about 30–50 s to converge and the diffusion is more than twice as fast. Compared to CASMO-5, the wall time of Tortin is 100 times lower and it only needs a few GB of memory. CASMO-5 needs more than 200 GB to run the ARI problem with the P3 scattering order. It is also interesting to notice that the computation times are about 30% lower for the controlled core than for the uncontrolled core because the convergence is reached after smaller number of iterations.

6. Results for quarter core depletion

6.1. Verification of Ventina against CASMO-5

As a first step before the coupling of Tortin and Ventina, a verification test was performed for the Ventina stand-alone solver, with fluxes taken from CASMO-5 as time averaged values from the beginning and the end of each depletion step. The calculated nuclide compositions were compared with the CASMO-5 ones and the differences for some important actinides and fission products of one pin cell of the uranium assembly with IFBA (the corner one) are shown in Fig. 10.

The compositions as calculated by CASMO-5 and Ventina agree in general very well. The error of ^{235}U concentration is within 0.1% even after reaching an average assembly burnup of 50 MWd/kg. The deviations of the main actinides are within 1.5% except for the very first burnup steps. However, at this early point in depletion, the nuclides densities of the minor actinides are extremely small, hence the errors caused on relevant quantities like the eigenvalue are negligible. The deviations for the most important fission products are mostly within 0.5%. There is about 1% error in ^{135}Xe concentration for the first burnup step of 0.1 MWd/kg but then the error decreases below 0.5%, so the impact on the eigenvalue should not be more than about 20 pcm. It should be mentioned here that CASMO-5 does not provide cross sections for the fission products for the zero burnup, so they have to be extrapolated. That could partly caused the differences between the two codes in the first burnup step. The error of the burnable absorber ^{10}B is slowly increasing, but it is almost completely burnt out after 10–15 MWd/kg.

6.2. History effect on SPH factors

More than 300 nuclides were explicitly tracked, which was found sufficient to describe the effect of spectral history on eigenvalue and power distribution, so the cross sections are not tabulated against the history variables. To evaluate the dependency of SPH factors on the spectral history, several lattice code calculations were done with non-nominal depletion and with branches for the nominal conditions. The SPH factors for these nominal branches were then compared with those obtained for the nominal depletion. As can be seen in Fig. 11, the difference is mostly small, except for the guide tube SPH factors after long operation with inserted control rods. Therefore, no correction of the SPH factors for the history variables is used.

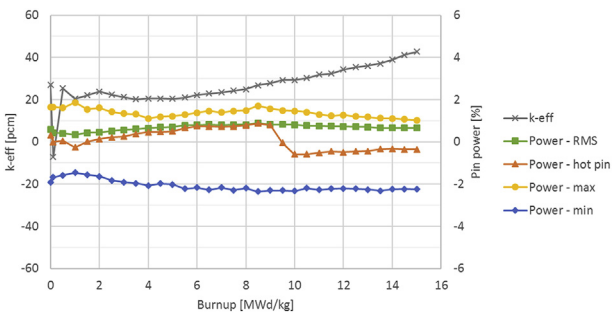

Fig. 12. Eigenvalue and pin power errors during nominal depletion.

6.3. Nominal depletion

In the first depletion test, the quarter core was depleted under nominal conditions, i.e. with constant temperatures, boron concentration, and under constant power, until reaching average burnup of 15 MWd/kg. The results are summarized in Fig. 12. During the whole depletion, the eigenvalue error is below 50 pcm and the pin power error RMS is below 1%. The maximum pin power error is about 2.2%, but it is located in a rod adjacent to the reflector corner where the power is small. The hot pin power error is small, with maximum of 0.9%. The power error maps for burnups of 0.1, 5, 10, and 15 MWd/kg are given in Fig. 13. They are mostly small, however the errors in the core center are increasing with burnup as the maximum power is moving from the core center towards the periphery, but they decrease again towards the end of the cycle.

6.4. Non-nominal depletion

In order to verify the coupling for a more challenging problem, we have designed several more complex depletion scenarios with non-nominal temperatures, decreasing boron concentration, non-nominal power or inserted control rods. When comparing the results with CASMO-5, the agreement was quite good, while the highest discrepancy was observed for long depletion with inserted control rods. This case is described in the following paragraph.

The core was depleted under nominal conditions until reaching the average burnup of 2 MWd/kg, then the control rods were inserted into 2 assemblies marked as G3 and C7 in the layout in Fig. 8. Moreover, the power was decreased to 50% of the nominal one, the fuel temperature was decreased by 100 K, the moderator temperature by 10 K, and the boron concentration was decreasing by 80 ppm per 1 MWd/kg. After reaching the burnup of 12 MWd/kg, the control rods were withdrawn, the power was set back to 100%, and the temperatures increased to the nominal ones. The boron concentration continued to decrease at the same speed.

The results are given in Figs. 14 and 15. The errors are in general small. The eigenvalue discrepancy is below 50 pcm and the pin power error RMS below 1% for almost all steps. The maximum errors are located around the reflector in the corner assemblies and are growing with the depletion up to 5.5%. There are also up to almost 6% errors in a few pins located next to the control rods at the moment of their removal. There are however quickly decreasing. The hot pin power error is mostly below 1% except for some time after the control rods removal, when the hot pins are located in the assemblies which were depleted with the control rods inserted.

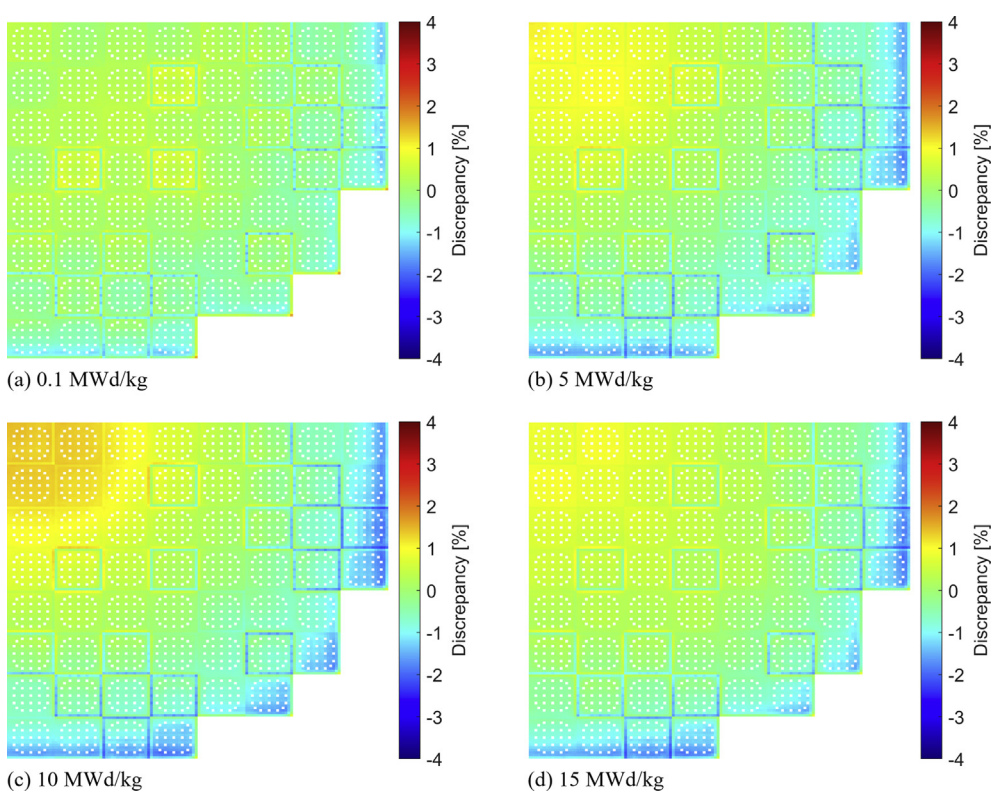

Fig. 13. Pin power error maps during nominal depletion.
(a) 0.1 MWd/kg (b) 5 MWd/kg
(c) 10 MWd/kg (d) 15 MWd/kg.

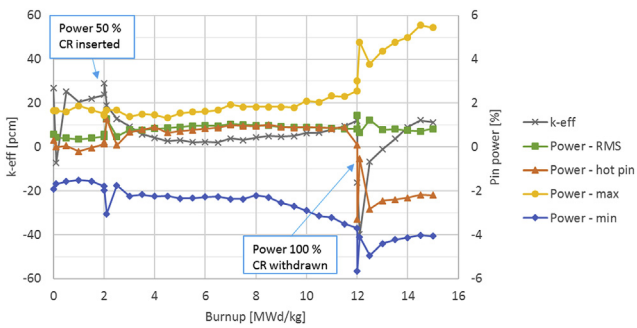

Fig. 14. Eigenvalue and pin power errors during non-nominal depletion.

7. Conclusion

This paper presents results obtained with a recently developed pin-by-pin code Tortin. Its SP3 solver with adequately produced cross sections can very well reproduce the lattice code solution even for very heterogeneous problems with MOX, assemblies with high burnup, and with inserted control rods. In the investigated 2D core with ARI, the pin power error RMS against the CASMO-5 reference solution obtained with Tortin SP3 was as little as 0.6%.

The Tortin solver requires diffusion coefficients calculated with the inscatter approximation, as the outscatter coefficient has been observed to cause several percent error in assemblies with high absorption and consequent lower power. The solver also requires reflector cross sections produced individually for each pin-size zone.

Regarding the spatial discretization, it was observed that the one mesh point per pin cell discretization in finite difference schemes, while being sufficient for most part of the fuel assembly, is not able to capture the rapid spectral flux changes on MOX/uranium or fuel/reflector interfaces. Therefore, an extended geometry mode was implemented, in which the two outer pin rows of each fuel assembly receive a finer, i.e. at least 2 meshes per pin cell discretization, yielding a significant reduction of interface errors, and not impairing the CPU time too much.

While the Tortin diffusion solver is about twice as fast as the SP3 solver, the diffusion solution is overall less accurate, especially for the controlled assemblies and for fuel with higher burnup, where diffusion tends to overpredict the pin power by 1–3%. Moreover, it significantly underpredicts the power in the two assembly rows adjacent to the baffle reflector by about 2%; this problem was, however, not observed for the water reflector.

Tortin was also coupled to a high-fidelity depletion solver Ventina. In the presented case, more than 300 nuclides are explicitly depleted. This set of nuclides should include all the actinides and fission products with significant impact on eigenvalue and power. Therefore, it was concluded that an additional correction of the macroscopic cross sections with branching calculations for history effects was not necessary anymore. It was also observed that the SPH factors are not strongly dependent on the history variables, hence no additional correction was used for them neither. The obtained pin-by-pin full core depletion results, even for strongly heterogeneous cores with MOX fuel, agree well with the full-core CASMO-5 reference ones. Even for a hypothetical reactor core depleted for almost the whole cycle with inserted control rods, the pin power error RMS staid mostly below 1% and the eigenvalue

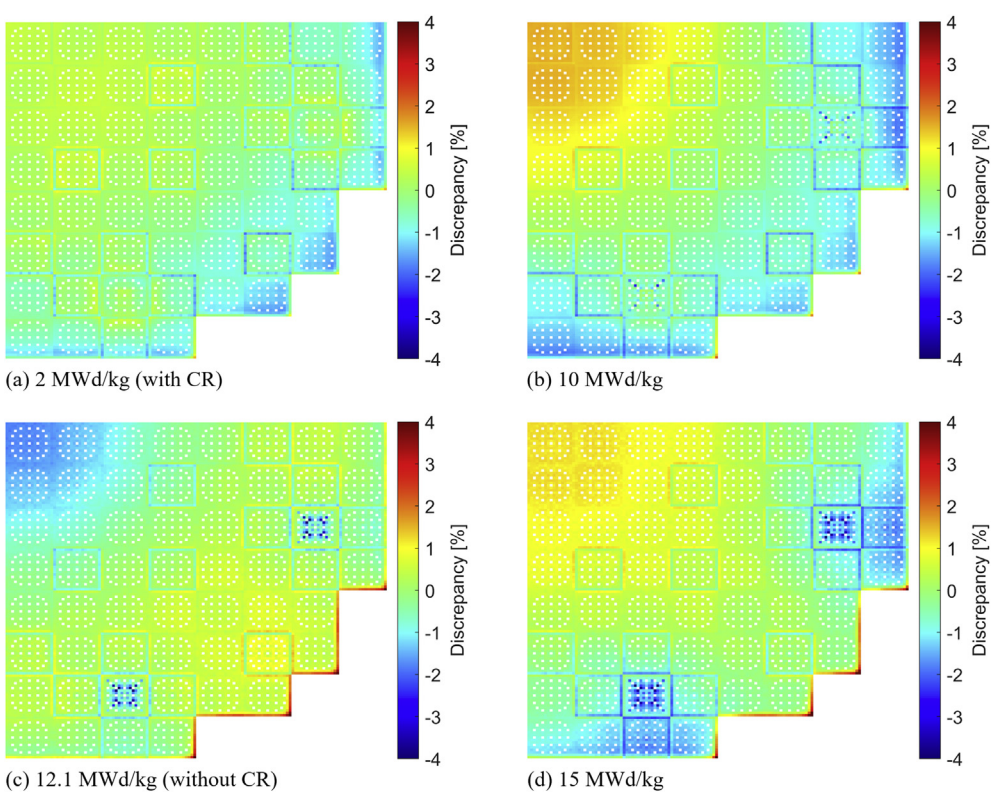

Fig. 15. Pin power error maps during non-nominal depletion.
(a) 2 MWd/kg (with CR) (b) 10 MWd/kg
(c) 12.1 MWd/kg (without CR) (d) 15 MWd/kg.

error below 50 pcm with respect to CASMO-5.

In the future, Tortin will be coupled with a subchannel thermal-hydraulic code and validated against measurements.

Declaration of competing interest

The authors declare that they have no known competing financial interests or personal relationships that could have appeared to influence the work reported in this paper.

Acknowledgments

This work was carried out in relation to the STARS project co-funded by ENSI, the Swiss nuclear regulator (H-101230).

Appendix A. Supplementary data

Supplementary data related to this article can be found at https://doi.org/10.1016/j.net.2020.04.022.

References

[1] T. Bahadir, S.-O. Lindahl, S. Palmtag, SIMULATE-4 multigroup nodal code with microscopic depletion model, in: M&C 2005, Avignon, France, 2005, pp. 12–15. September.
[2] A. Dall'Osso, D. Tomatis, Y. Du, Improving cross sections via spectral rehomogenization, in: PHYSOR 2010, Pittsburgh, Pennsylvania, USA, 2010. May 9-14.
[3] A. Yamamoto, M. Tatsumi, Y. Kitamura, Y. Yamane, Improvement of the SPH method for pin-by-pin core calculations, J. Nucl. Sci. Technol. 41 (2010) 1155–1165.
[4] T. Kozlowski, Y. Xu, T.J. Downar, D. Lee, Cell homogenization method for pin-by-pin neutron transport calculations, Nucl. Sci. Eng. 169 (2011) 1–18.
[5] A. Seubert, Pin cell discontinuity factors in the transient 3-D discrete ordinates code TORT-TD, in: PHYSOR 2010, Pittsburgh, Pennsylvania, USA, 2010. May 9-14.
[6] A. Calloo, S. Huy, D. Couyras, C. Brosselard, M. Fliscounakis, Validation of the SPn depletion schemes of the EDF GABV2-COCAGNE tools using the KAIST 1A benchmark, in: PHYSOR 2016, Sun Valley, Idaho, 2016. May 1-5.
[7] N. Garcia-Herranz, D. Cuervo, A. Sabater, G. Rucabado, S. Sanchez-Cervera, E. Castro, Multiscale neutronics/thermal-hydraulics coupling with COBAYA4 code for pin-by-pin PWR transient analysis, Nucl. Eng. Des. 321 (2017) 38–47.
[8] M. Daeubler, N. Trost, J. Jimenez, V. Sanchez, R. Stieglitz, R. Macian-Juan, Static and transient pin-by-pin simulations of a full PWR core with the extended coupled code system DYNSUB, Ann. Nucl. Energy 84 (2015) 31–44.
[9] D.W. Dean, SIMULATE-3 – Advanced Three-Dimensional Two-Group Reactor Analysis Code vol. 4, 2007. Studsvik Scandpower report SSP-95/15-Rev.
[10] C. Lee, Y. Kim, J. Song, C. Park, Incorporation of a new spectral history correction method into local power reconstruction for nodal methods, Nucl. Sci. Eng. 124 (1996) 160–166.
[11] F. Hoareau, E. Girardi, C. Brosselard, M. Fliscounakis, Verification of the COCAGNE core code using cluster depletion calculations, in: PHYSOR 2014, Kyoto, Japan, 2014. September 28 – October 3.
[12] The ARCADIA Reactor Analysis System for PWRs Methodology Description and Benchmarking Results, 2010. ANP-10297NP, Rev. 0.
[13] P. Mala, A. Pautz, H. Ferroukhi, EPR fuel cycle depletion with pin-by-pin code Tortin and nodal code SIMULATE5, in: M&C 2019, Portland, Oregon, USA, 2019. August 25-29.
[14] M. Zilly, J. Bousquet, K. Velkov, A. Pautz, PWR cycle analysis with the GRS core simulator KMACS, Jahrestagung Kerntechnik, Berlin, Germany, 2018, pp. 27–30. May.
[15] Intel Math Kernel Library, Developer reference, 2018.
[16] Fast Auxiliary Space Preconditioning, 2019 downloaded from, https://fasp.sourceforge.net.
[17] J. Rhodes, K. Smith, D. Lee, CASMO-5 development and applications, in: PHYSOR 2006, Vancouver, Canada, 2006. September 10-14.
[18] S. Choi, K. Smith, H. Lee, D. Lee, Impact of inflow transport approximation on light water reactor analysis, J. Comput. Phys. 299 (2015) 352–373.
[19] Z. Liu, K. Smith, B. Forget, A cumulative migration method for computing rigorous transport cross sections and diffusion coefficients for LWR lattices with Monte Carlo, in: PHYSOR 2016, Sun Valley, Idaho, 2016. May 1-5.
[20] J. Leppanen, M. Pusa, E. Friedman, Overview of methodology for spatial homogenization in the Serpent 2 Monte Carlo code, Ann. Nucl. Energy 96 (2016) 126–136.
[21] B.R. Herman, B. Forget, K. Smith, B.N. Aviles, Improved diffusion coefficients generated from Monte Carlo codes, in: M&C 2013, Sun Valley, USA, 2013. May 5-9.
[22] A. Hebert, A consistent technique for the pin-by-pin homogenization of a pressurized water reactor assembly, Nucl. Sci. Eng. 113 (1993) 227–238.
[23] S.-O. Lindahl, T. Bahadir, G. Grandi, SIMULATE5 – Methodology, 2011. Studsvik Scandpower Report SSP-10/465.
[24] T. Clerc, A. Hebert, H. Leroyer, J.-P. Argaud, A. Poncot, B. Bouriquet, Presentation of the MERC work-flow for the computation of a 2D radial reflector in a PWR, in: M&C 2013, Sun Valley, USA, 2013. May 5-9.
[25] M. Pusa, J. Leppanen, Computing the matrix exponential in burnup calculations, Nucl. Sci. Eng. 164 (2010) 140–150.
[26] M. Pusa, Rational approximations to the matrix exponential in burnup calculations, Nucl. Sci. Eng. 169 (2011) 155–167.
[27] T. Kozlowski, T.J. Downar, Pressurised Water Reactor MOX/UO2 Core Transient Benchmark, 2006. NEA/NSC/DOC(2006)20.